# The Jetting Phenomena in Meshed Spur Gears

**Irebert Delgado**
Mechanical Engineer
NASA
Cleveland, OH, USA

**Michael Hurrell**
Aerospace Engineer
HX5 Sierra, LLC/TFOME II
Cleveland, OH, USA

## ABSTRACT

Rotorcraft gearbox transmissions are required to efficiently transfer power from the turbine engine to the main and tail rotor blades. Losses in transmission efficiency impact mission payload and aircraft range. These systems are expected to deliver high power with high gear pitch line velocities. More recently, shrouding has been employed to reduce windage power losses associated with the high gear rotational speeds. However, recent experimental results from tests conducted by the authors show the negative impact of close clearance shrouds on windage power loss, particularly at the meshed region where flow is ejected, or jetted, from the collapsing tooth spaces. A literature review was conducted to gain further insight into the phenomenon of gear mesh jetting and strategies to mitigate and control the associated losses. An analysis was conducted on windage losses in the mesh region. Test results are given for a modified shroud configuration. Finally, a discussion on observed trends follows with suggestions on future research.

## INTRODUCTION

Losses in geared systems can be divided into load-dependent and load-independent losses. Load-dependent losses are losses incurred in the gears and bearings which increase proportionally with applied load. Load-independent losses or spin-losses, as described by Kahraman and others in Ref. 1, are those losses incurred without an applied load. Gear windage power losses (WPL) are categorized under spin losses and are composed of, i) viscous drag on the faces of the gear, ii) impingement of the air/oil medium on the gear teeth, also known as pressure torque (Ref. 2), and iii) pumping of the air/oil medium in the inter-tooth spaces of the gear. High velocity jetting is believed to occur during the 'engaging' portion of the meshing cycle for a pair of spur gear teeth in mesh. In general WPL has been found to significantly affect gearbox efficiency above 10,000 ft/min (Refs. 3-4).

Researchers have found that the use of shrouding can mitigate viscous and pressure torque drag losses. For spur gears, shrouding involves enclosing the component axially and radially with strategically placed drain holes. Hill (Ref.2) and others have shown through computational fluid dynamic (CFD) analysis that shrouding acts to preserve the fluid velocity at the vicinity of the rotating gear resulting in reduced power consumption. In general, WPL is reduced with decreasing clearance between the stationary shroud and the rotating gear. However, recent results from tests conducted on shrouded meshed spur gears by Delgado and Hurrell given in Ref. 5 show that the beneficial effects of shrouding may be offset by axial jetting in the vicinity of the gear mesh. Figure 1 shows WPL results for different shroud configurations for a pair of meshed spur gears. The experiment was conducted at NASA Glenn Research Center's gear windage test rig, Figure 2. From previous research, the small-axial, small radial clearance should give the largest reduction in WPL. However, the largest reduction in WPL is given by the large axial, small radial clearance configuration. Assuming that jetting exists at the spur gear mesh and was 'blocked' by the close clearance shroud (e.g. small-axial, small-radial clearance data), the air/fluid medium could be redirected back towards the gear faces as well as inter-tooth spaces, thereby increasing WPL.

To gain a better understanding of and to possibly control the jetting phenomena, especially with the use of shrouding, a literature search was conducted to answer a series of questions:

1) What is the underlying physical mechanism causing the axial jetting in meshed spur gears?

2) What analyses and experiments have been conducted?

3) How is jetting related to squeezing and pocketing power losses?

4) How is efficiency affected in transmitting power?

5) How does axial jetting affect the use of shrouding?

A windage loss analysis is conducted followed by test results of a modified shroud configuration. This is followed by a discussion on observed trends, open issues, and suggestions for further work.

Presented at the AHS International 74th Annual Forum & Technology Display, Phoenix, Arizona, USA, May 14-17, 2018.

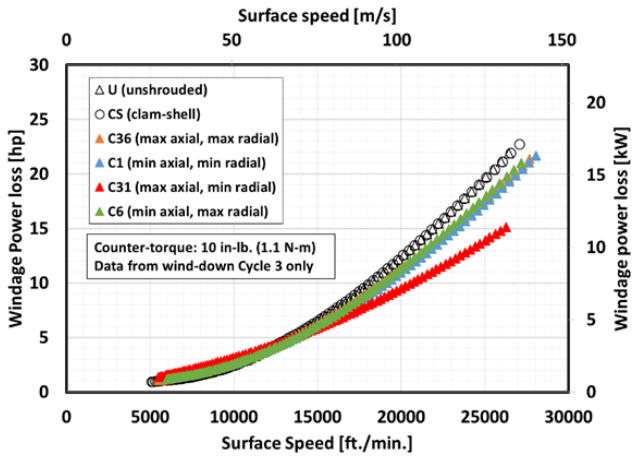


**Figure 1 Comparison of meshed spur gear windage power loss versus shroud configuration clearances.**

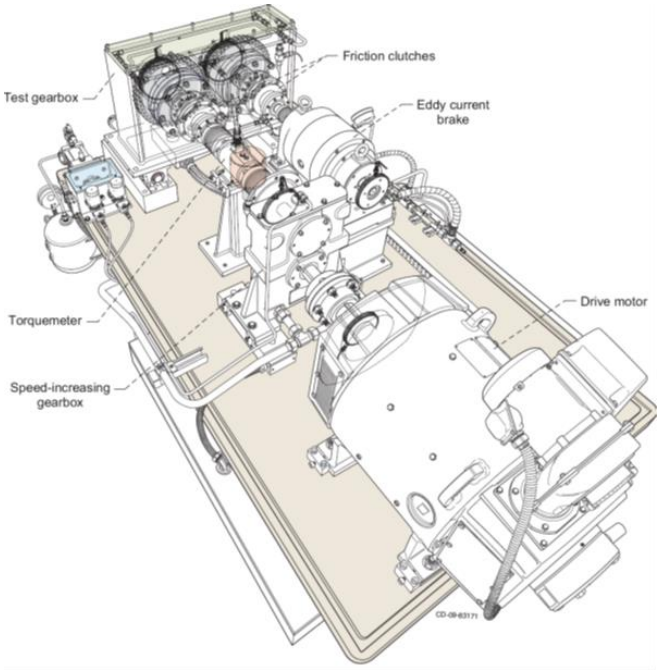


**Figure 2 NASA Glenn Research Center gear windage test rig**

## LITERATURE REVIEW

In efforts to decrease noise or reduce power losses in geared systems, several researchers have theorized, modeled, or observed the air/oil medium being squeezed out of the spaces between meshed spur gear teeth. Following is a review of the findings of those researchers with emphasis on the questions noted above and more specifically, for this study, how it impacts the effectiveness of shrouding in reducing windage power loss.

**What is the underlying physical mechanism causing the axial jetting in meshed spur gears?**

Early acoustic experiments by Rosen published in 1961 (Ref. 6) point to air being forced out of the space between a gear tooth and its mating gear teeth. Dudley in Ref. 7 notes that oil may become trapped in the meshing region resulting in power loss and "to allow for plenty of room within the casing" to possibly mitigate this effect. Wittbrodt and Pechersky (Ref. 8) describe the phenomenon as the air and lubricant in the volume space between mating teeth being compressed and forced out of the 'sides' and 'between' the mating teeth. Diab (Ref. 9) describes the phenomena as a trapping of the air/oil mixture in the tooth interspaces as it undergoes a compression and expansion within a tooth meshing cycle. The gas can flow in both the axial and radial directions. Seetharaman et al. (Ref. 10) describe the phenomenon as 'pocketing' where the air/oil mixture is treated as a compressible fluid confined by the cavity making up a tooth on one gear and the mating space between two adjacent teeth on the opposing gear, or inter-tooth space. Due to rotation, the volume of air/oil is squeezed resulting in a higher pressure differential than outside the volume. The mixture is forced out of the ends and backlash regions of the inter-tooth cavity.

**What analyses and experiments have been conducted?**

Analyses by Rosen in Ref. 6 calculate air discharge velocities for the spur gear meshing region based on change in volume as the teeth rotate through mesh. His findings show that the maximum discharge velocity occurred at nearly the same time as the measured maximum acoustic energy. For the gear geometry tested, this maximum velocity occurs approximately 8 degrees before contact at the pitch point. Additionally, it is noted that air is discharged prior to the pitch point and then "sucked in" after the pitch point. Finally, one of the methods used to quiet the gears was to allow a large space at the 'two ends' of the teeth for air and oil to escape. For the gear geometry tested, Rosen calculates discharge velocities approaching sonic conditions.

Published work in 1973 by Ariura and others (Ref. 11) models power loss due to oil 'trapping' and 'acceleration'. Power loss due to trapping of the oil was found to be significant at flow velocities of 10-20 m/s (1969-3937 ft/min) while power loss values due to circumferential acceleration of the oil was significant at higher velocities. Experimentally, jetted lubricating oil was also observed to flow axially out of the meshing region.

Wittbrodt et al. in 1987 (Ref. 8) performs a one-dimensional incompressible and compressible flow analysis that shows higher fluid flow at the gear tooth tips compared to axial flow at the ends of the gear teeth. Fluid velocities may reach sonic conditions and is dependent on rotational speed and relative gear geometries. Peak velocities are shown to occur

prior to the gear teeth reaching their pitch point in the meshing cycle and again varies with geometry. Regarding the specific rotational position of maximum end flow, positive or negative, Wittbrodt's analysis provides a number of factors that affect this location. Higher pitch-line velocities, smaller backlash, and larger gear ratio tend to move the maximum velocity earlier in the meshing cycle. One particular interesting result shows non-dimensional velocity going to zero just after the pitch point. Recall that Rosen's work shows air velocities becoming negative after the pitch point, indicating a reversal in fluid flow from expulsion to ingestion. While not explicitly discussed by Wittbrodt, several other researchers (Ref. 6, 9, 10) report negative fluid velocities after the meshing spur gears pass the pitch point (i.e. fluid ingestion into the gear tooth spaces). Additional trends from Wittbrodt's analysis include the following:

1) Tooth flow velocities are generally higher than end flow velocities
2) End flow tends to dominate narrow face width gears.
3) Higher fluid velocities result from spur gears with ratios closer to unity.
4) Higher fluid velocities result from smaller backlash.
5) Higher fluid velocities result from higher pitch-line velocities.
6) Higher pitch-line velocities shift the peak fluid velocity (possibly sonic) to earlier in the meshing cycle.

Using conservation of momentum principles, Seetharaman in Ref. 10 calculates discharge velocities at the ends and backlash regions of mating spur gear teeth. Results show that end flow power loss increases with respect to backlash power loss as face width increases, corroborating findings by Wittbrodt et al. (Ref. 8) Analyses show a maximum positive velocity (i.e. expulsion) prior to the pitch point and a maximum negative velocity (i.e. suction) after the pitch point. The absolute magnitude of these velocities increases with increasing pitch-line velocity. For the unity ratio gears analyzed, end flow pressures increased with increasing velocity. End flow pressure magnitudes were slightly less than the magnitudes of the backlash pressure. Correspondingly, end flow velocities were slightly lower than backlash flow velocities for a given rotational position.

A CFD analysis in a fully immersed lubricating fluid by Concli et al. (Ref. 12) shows that the axial velocity at the gear mesh is maximum in the middle of the width of the tooth and decreases rapidly towards the end (opening) of the mating teeth.

Al et al. (Ref. 13) performs a single phase 2-D modelling study on meshed spur gears. The mesh between the gear teeth is modelled as they go into and out of mesh. Contact between the gear teeth is not modelled. Axial flows are not considered in the model. Results support the existence of a maximum positive pressure prior to the meshing pitch point. The results also support that a period of expulsion (positive flow) exists prior to the meshing pitch point followed by a period of suction (negative flow) after the meshing pitch point. Results are in agreement with experimental data by Diab et al. (Ref. 9).

Burberi et al. (Ref. 14) simulates meshed spur gears rotating in a submerged oil with the flow modelled as isothermal and incompressible. A dynamic mesh moving boundary approach is used with gear teeth not in contact (i.e. 2/3 element fluid layer). Results are comparable with experiments by Gorla et al. (Ref. 15). Results show oil flow moving out of and into mesh.

Experimental and analytical work by Diab et al. (Ref. 9) show a positive increase in pressure at the root of the gear teeth during meshing but a rotational angle before the pitch point. This is followed by a decrease in pressure (i.e. suction) after the pitch point. The analysis and observations are in line with those of Rosen (Ref. 6), Wittbrodt (Ref. 8), and Seetharaman (Ref. 10).

Particle image velocimetry (PIV) studies by Hartono et al. (Ref. 16-17) for meshed spur gears at different levels of oil immersion show recirculation of fluid flow that impinge on the sides and faces of the gear teeth. Pitch-line velocities were limited to less than 20 m/s (3937 ft/min). Visual analysis in a fully immersed condition at 0.55 m/s (108 ft/min) and 1.1 m/s (217 ft/min) gear pitch-line velocity indicated fluid movement into mesh. The particle trajectories, or streamlines, in the vicinity of the meshing region show an axially outward flow that increases in intensity with pitch line velocity.

As shown in Figure 1, Delgado and Hurrell (Ref. 5) observe that the maximum axial, minimum radial shroud configuration gives a lower windage power loss than the minimum axial, minimum radial shroud configuration. One possible reason for this result is the recirculation back into the meshing/rotational region of the axial jetting mixture.

**How is jetting related to squeezing and pocketing power losses?**

For the purposes of this study, jetting is the axial flow of fluid resulting from the squeezing, or pocketing, of that fluid mixture (air and oil) in the volumetric interspaces of the meshed spur gears. Generally, jetting occurs in the first half of the meshing cycle between a pair of mating spur gear teeth prior to those teeth reaching the pitch point. For compressible fluids, the sharp decrease in volumetric space results in an expulsion of fluid axially out of the ends of the meshed spur gear teeth and radially through the backlash region. The compression of fluid and flow out of the volume results in power loss. Jetting and the associated power loss can be affected by the placement of axial shrouds.

**How is efficiency affected in transmitting power and how does axial jetting affect the use of shrouding?**

Several researchers (Refs. 3-5) have noted that windage power loss (WPL) becomes increasingly problematic above

10,000 ft/min. The use of shrouds in Ref. 18 by the authors has been shown to decrease WPL for meshed spur gears. Analyses by researchers at The Pennsylvania State University (Ref. 2) show the largest decrease in WPL for single spur gears using shrouds at close clearance. Although the use of close clearance shrouds for meshed spur gears resulted in a decrease in WPL, it did not translate into the largest decrease in WPL. The largest decrease in WPL was observed using the large axial, small radial shroud configuration, Figure 1. Comparing this data with PIV data by Hartono et al. (Refs. 16-17) as well as analyses on the jetting phenomena from several researchers, we conclude that axial jetting would need to be better controlled particularly at high speeds. Table 1 summarizes the analyses and experiments found regarding the axial jetting phenomena.

**Table 1 Summary of data sources for axial jetting phenomena.**

| Source | Analytical | Experimental | Notes |
|---|---|---|---|
| Rosen (Ref. 6) | Change in volume | Acoustic, noise | |
| Ariura et al. (Ref. 11) | n/a | Axial jetting observed via stroboscope | |
| Wittbrodt et al. (Ref. 8) | 1-D incomp. and compressible | n/a | |
| Seetharaman et al. (Ref. 10) | closed-form, compressible, phys.-based | Compare to data from (Ref.19) | Single phase fluid |
| Concli et al. (Ref. 12) | 3-D CFD, VOF | n/a | Oil bath, no tooth contact |
| Al et al. (Ref. 13) | 2-D CFD | n/a | 1-phase, no tooth contact |
| Burberi et al. (Ref. 14) | 3-D CFD, incomp. | n/a | |
| Diab et al. (Ref. 9) | Isentropic, numerical | Gear tooth root pressure measurement | Air only |
| Hartono et al (Refs.16-17) | n/a | PIV | |
| Delgado et al. (Ref. 5) | n/a | Gear windage power loss | |

**Analysis of Literature Survey**

Analyses by Rosen (Ref. 6), Wittbrodt (Ref. 8), and Seetharaman (Ref. 10) indicate a maximum positive end flow velocity prior to the teeth of two meshed spur gears reaching the pitch point in the meshing cycle. This is followed by a maximum negative end flow velocity after reaching the pitch point, Figure 3 and Figure 4. Experimental work by Diab et al. (Ref. 9) corroborate these findings through experimental observation. The trapped volume between the meshed gears decreases to a minimum at the pitch point, then expands afterwards. For incompressible flows, Wittbrodt et al. (Ref. 8) found that the highest fluid velocities occurred when discharge areas, end flow or tooth flow, were minimal and volume changes with respect to rotational position where maximized. A number of results indicate discharge velocities approaching sonic conditions.

Although the Hartono (Refs. 16-17) study did not specifically show an axial jetting fluid flow component, the increased outward bow around the meshing region when comparing the data at 0.55 m/s (108.3 ft/min) and 1.1 m/s (216.5 ft/min) may be an indication of increased influence of that phenomena on the local flow field. This agrees with previous research findings that axial jetting velocities increase with increasing pitch-line velocities. Given that the authors conducted windage power loss tests with jet-lubricated gears at pitch-line velocities near 150 m/s (29,500 ft/min), the axial jetting velocities could be substantial.

Nearly all research noted above indicate that maximum end flow velocities were attained prior to reaching the pitch point for any pair of meshed spur gear teeth in the meshing cycle. An open question is where is that maximum velocity relative to the ‘center distance’ direction between meshed spur gears. For involute gear tooth profiles, the line of action is a straight line as shown in Figure 3 and defines the tooth contact for the entire meshing cycle for a pair of spur gear teeth. Also, depending on the gear rotation, the line of action is skewed either to the right or left relative to center. These observations should be accounted for, assuming close clearance shroud designs are diverting the air/lubricant flow back to the meshing and rotational regions. Note also, for non-involute gear tooth profiles the line of action may be an S-curve (Ref. 20). A number of researchers have also noted a suction effect after any pair of meshed spur gears have reached the pitch point. The end flow is reversed, going into mesh instead of out-of-mesh. Its effect on windage power loss, if any, is unknown, with or without shrouding.

In terms of exit velocities, Rosen and Wittbrodt’s analyses for their particular meshed spur gear geometries show axial velocities approaching sonic conditions. In addition, higher pitch-line velocities result in the exit velocity reaching sonic conditions earlier in the meshing cycle. Higher pitch-line velocities are also known to increase windage power loss.

A number of researchers show backlash velocities slightly higher than end flow velocities. Its effect on windage power loss is unknown. It may be reasonable to assume that any type of air/oil flow back into the meshing region would have a negative effect on windage power loss. Modeling and experiment using a shroud design that blocks the suction flow into the gear mesh would improve understanding of the

flow in this portion of the meshing cycle. Given findings that exit flows reach nearly sonic conditions combined with visualization studies by Hartono, further analyses and experiments are needed to determine if the flow is axially straight relative to the meshing region or, alternatively, its direction is dependent on rotational speed, gear tooth geometry, etc.

Although the Hartono study was done at relatively low pitch-line velocities, the visualization results indicate fluid flow near the meshing region as axially outward and down (i.e. towards the out-of-mesh region). The direction of the fluid flow was, up to this point, assumed to be axially outward and orthogonal to the meshing region. Additional work is needed to corroborate these results.

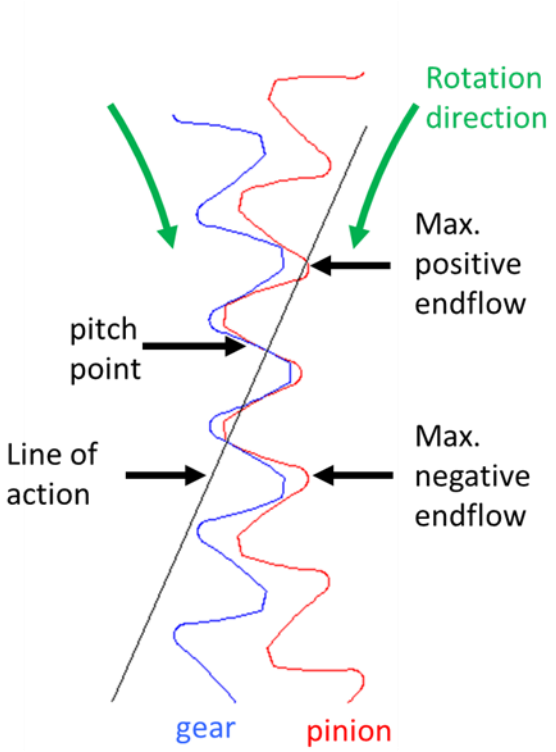


**Figure 3 Relative positions of maximum positive and negative end flow per literature review for meshed spur gears.**

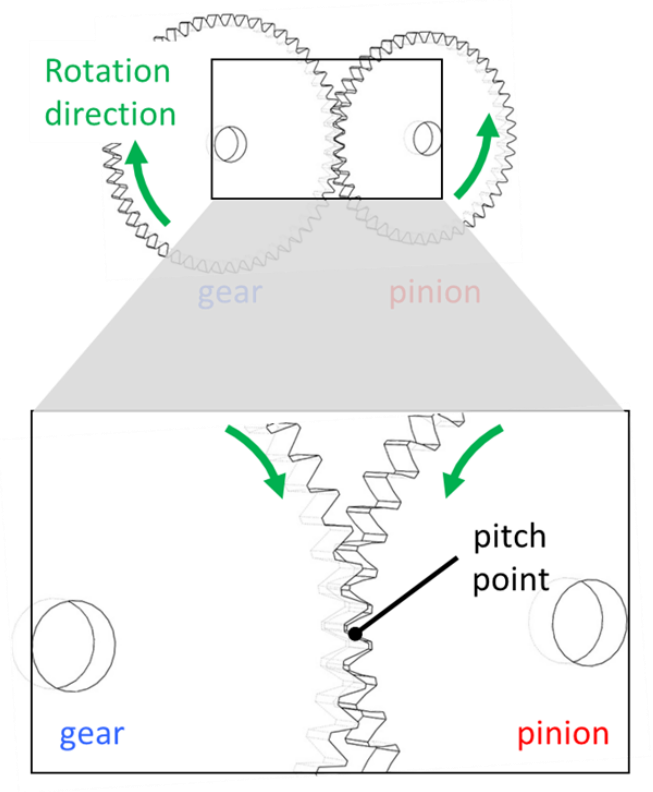


**Figure 4 Meshed spur gears showing trapped volume decreasing and increasing in magnitude prior and after the pitch point.**

## POCKETING CALCULATION

Referring to the recent results from tests conducted on shrouded meshed spur gears given in Ref. 5, an analysis was conducted to determine the power loss due to pocketing of the test gears. The test results indicate that axial shrouding may have an adverse effect on windage power loss as a result of pocketing and associated axial jetting in the vicinity of the gear mesh. The literature suggests an approach to estimating the power loss associated with pocketing (Refs. 6, 8, 9, & 10). The approach involves defining the control volume created by the meshing action and applying the conservation laws to the control volume at time instants during the mesh cycle.

During the first half of the mesh cycle, the meshing action creates pockets of trapped volume that contain a mixture of air and oil. The trapped volumes decrease in size and shape during the first half of the mesh cycle. The decreasing volume results in flow axially out of the two ends of the volume and radially through the space created by the backlash of the mating gears. Since the loss mechanism associated with the end flow is closely affected by the positioning and configuration of axial shrouds, the proceeding analysis focusses on that portion of pocketing power loss attributed to end flow, i.e. axial jetting.

Following the volume created by the tooth space on the driven gear and the mating tooth of the drive gear, two control volumes can be defined at time $t_1$ and time $t_2$ as shown in Figure 5. Two corresponding volumes are formed by the tooth space on the drive gear and the mating tooth of the driven gear (not shown). The volume changes shape and size as the mesh cycle progresses. The volume size decreases as the two gears proceed through the mesh cycle and reaches a minimum at the pitch point. After the pitch point, the volume begins to increase until the two gears proceed out of mesh.

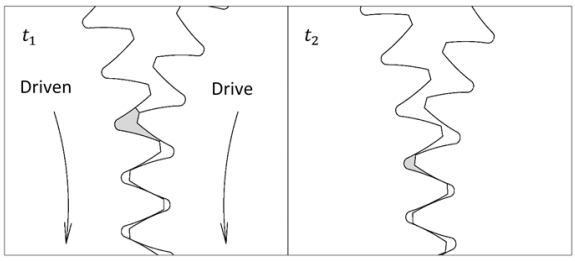


**Figure 5 Control volume change from time $t_1$ to $t_2$ during the meshing cycle.**

Referring to the first half of the mesh cycle where the volume is decreasing, the control volumes ($V^{(1)}$, $V^{(2)}$) and flow areas for times $t_1$ and $t_2$ are defined as shown in Figure 6.

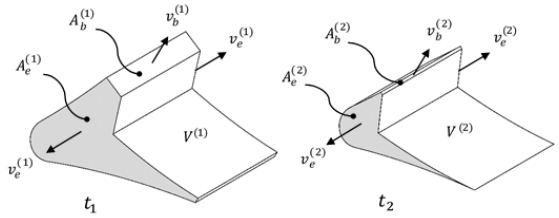


**Figure 6 Control volume at $t_1$ and $t_2$.**

The backlash area and end areas at time $i$ are given as $A_b^{(i)}$, and $A_e^{(i)}$ respectively. Likewise, the backlash velocity and end velocities are $v_b^{(i)}$, and $v_e^{(i)}$. From conservation of mass, the time rate of change of mass in the control volume plus the net mass efflux crossing the control surface is zero.

$$\frac{d}{dt}\int_{cv} \rho_{cv} dV + \int_{cs} \rho \boldsymbol{v} * \boldsymbol{n} dA = 0 \tag{1}$$

Proceeding from time $t_1$ to time $t_2$, this relation can be discretized with respect to time.

$$\frac{1}{\Delta t}\left[{\rho_{cv}}^{(2)} V^{(2)} - {\rho_{cv}}^{(1)} V^{(1)}\right] + 2\rho_e^{(1)} v_e^{(1)} A_e^{(1)} + \rho_b^{(1)} v_b^{(1)} A_b^{(1)} = 0 \tag{2}$$

The control volume density and the densities at the backlash area and end areas at time $i$ are given by $\rho_{cv}^{(i)}$, $\rho_b^{(i)}$, and $\rho_e^{(i)}$. Rearranging shows that the velocities are related to the change in volume from $t_1$ to $t_2$.

$$2\rho_e^{(1)} v_e^{(1)} A_e^{(1)} + \rho_b^{(1)} v_b^{(1)} A_b^{(1)} = -\frac{1}{\Delta t}\left[{\rho_{cv}}^{(2)} V^{(2)} - {\rho_{cv}}^{(1)} V^{(1)}\right] \tag{3}$$

Assuming the backlash velocity is proportional to the end velocity

$$v_b = a v_e \tag{4}$$

where $a$ is the proportionality constant and the time increment $\Delta t$, from $t_1$ to $t_2$, is related to the gear surface speed $v_s$

$$\Delta t = \frac{\Delta\theta}{\omega} = \frac{r\Delta\theta}{v_s} \tag{5}$$

then Equation 3 can be rewritten for the end velocity.

$$v_e^{(1)} = -\frac{v_s}{r\Delta\theta}\left[\frac{\rho_{cv}^{(2)} V^{(2)} - \rho_{cv}^{(1)} V^{(1)}}{2\rho_e^{(1)} A_e^{(1)} + a\rho_b^{(1)} A_b^{(1)}}\right] \tag{6}$$

The gear angular speed, the angular increment from $t_1$ to $t_2$ and the gear pitch radius are given by $\omega$, $\Delta\theta$, and $r$ respectively. Note that the end and backlash velocities are relative velocities since the frame of reference is rotating with the gear.

As shown in Equation 6, the end velocity is non-linearly related to the surface speed of the mating gears. Using the relations above, the end velocities for the NASA test spur gears were calculated for various pitch line velocities up to 46,077 ft/min corresponding to the maximum test rig speed of 16000 rpm. The results of these calculations for a particular angular position that corresponds to the first ¼ of the mesh cycle are shown in Figure 7. Results for the NASA test gears show that by the time ¼ of the mesh cycle is complete, the end velocity reaches sonic velocity at a surface speed of 46,077 ft/min. In addition, the relations above show that an increase in pitch line velocity results in a decrease in the time to reach sonic end velocity and correspondingly an earlier occurrence of sonic end velocity in the mesh cycle.

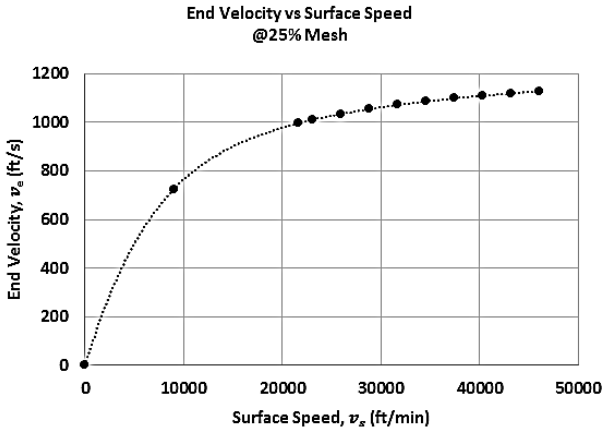


**Figure 7 End velocity versus surface speed for the NASA spur gears.**

From conservation of linear momentum, the total force acting on the control volume is the time rate of change of linear momentum within the control volume plus the net efflux of linear momentum crossing the control volume surface.

$$\sum \boldsymbol{F} = \frac{d}{dt}\int_{cv} \rho_{cv} v_{cv} dV + \int_{cs} \rho_{cs} \boldsymbol{v}_{cs} \boldsymbol{v}_{cs} * \boldsymbol{n} dA \qquad (7)$$

The force acting on the volume end areas is related to the end velocity

$$F_e = \rho_e (v_e)^2 A_e \qquad (8)$$

Since there are two end areas, then the power loss due to axial jetting is given as

$$P_e = 2 v_e F_e \qquad (9)$$

and substituting Equation 8 gives

$$P_e = 2\rho_e (v_e)^3 A_e \qquad (10)$$

The pocketing power loss due to axial jetting varies with the end velocity cubed and for high pitch line velocities, the end velocity can approach the speed of sound.

Seetharaman, et al. (Ref. 10) breaks the total windage power loss of two spur gears in mesh into two components; pumping loss due to pocketing $P_p$, and loss due to drag $P_d$.

$$P_w = P_p + P_d \qquad (11)$$

The pumping power loss due to pocketing is further subdivided into the power loss from end flow $P_e$, and power loss from backlash flow $P_b$. Seetharaman also divides the drag component into two subcomponents; drag on the drive gear $P_{d1}$, and drag on the driven gear $P_{d2}$. Calculations of the pocketing power loss at drive gear surface speeds in excess of 25,000 ft/min for the NASA test gears and test results for different shroud configurations of both single and meshed spur gears (Ref. 5) indicate that a large portion of the total windage power loss is unaccounted for based on the pocketing and drag formulations defined above. Percentages of the total power loss at 25,000 ft/min for the unshrouded meshed spur gear test (largest radial and largest axial shroud clearance) and the C1 shroud configuration meshed spur gear test (smallest radial and smallest axial shroud clearance) reported in Ref. 5 are shown in Figure 8 and Figure 9, respectively. Seetharaman reported a similar discrepancy between predicted and experimental total windage power loss at higher gear speeds.

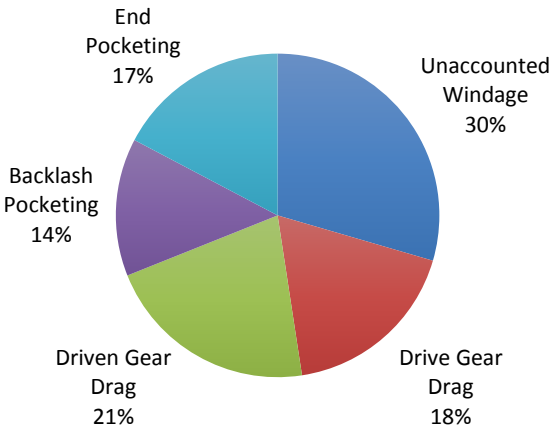


**Figure 8 Total windage loss component percentages for the unshrouded test condition (largest radial and largest axial shroud clearance) at 25,000 ft/min drive gear surface speed.**

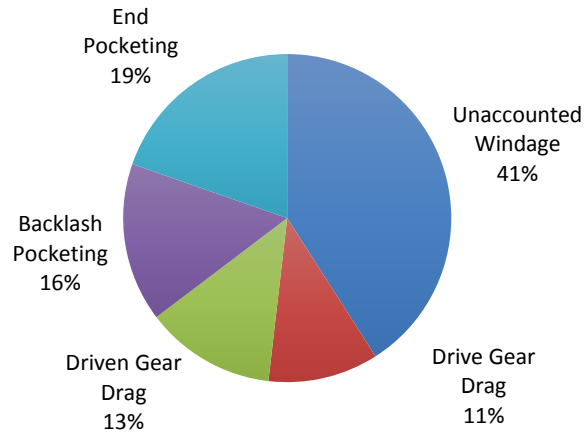


**Figure 9 Total windage loss component percentages for the C1 shroud configuration (smallest radial and smallest axial shroud clearance) at 25,000 ft/min drive gear surface speed.**

Comparing the results from testing conducted at NASA of shrouded single and meshed spur gears shown in Figure 10 and Figure 11 respectively indicate that there may be a third subcomponent of drag related to the interaction of the two gears in the vicinity of the mesh region $P_{d12}$.

$$P_d = P_{d1} + P_{d2} + P_{d12} \qquad (12)$$

The flow in this region is highly turbulent and is the result of the impingement of the flows attached to the two gears as they rotate in opposing directions.

Hill (Ref. 2) performed a CFD analysis of the NASA spur gears and observed vortices in the tooth space of the gears when enclosed in a radial shroud. This secondary flow may be another mechanism of loss contributing to total windage

power loss. The vortices in the tooth space are similar to the flow within the flow passages of a periphery, or regenerative pump. A regenerative pump is used in large head, small flow applications that are not suited for the traditional centrifugal or positive displacement pump (Ref. 21). The testing conducted at NASA indicates that this secondary flow may be present for the case of tight clearance radial shrouding. As a result, a third component of pumping power loss $P_s$, due to this secondary flow within the gear tooth space for close radial shrouding can be added to the pumping power loss due to pocketing.

$$P_p = P_e + P_b + P_s \tag{13}$$

The NASA tests (Ref. 5) indicate that closely conforming axial and radial shrouds can reduce total windage power loss. However, these tests also indicate that an optimized shroud configuration requires a closer examination of the component loss mechanisms that contribute to the total windage power loss and determining how these mechanisms are affected by shrouding. For instance, close axial shrouds may help in reducing drag loss on the sides of the gears but may increase losses due to pocketing. Close clearance axial shrouds may act to reduce the flow through the two end areas $A_e$, forcing more of the compressed pocket volume to squeeze through the smaller backlash area $A_b$, resulting in an increase in pocketing loss. For close clearance radial shrouds, the study by Hill (Ref. 2) shows the presence of secondary flows within the tooth spaces of the NASA spur gears. This secondary flow may contribute to the overall pumping power loss when close radial shrouding is utilized. The NASA tests are inconclusive with regards to the effect of shrouding on the drag loss associated with the interaction of two gears in mesh $P_{d12}$. This loss mechanism may follow the same trend as the individual gear drag loss components $P_{d1}$ and $P_{d2}$; i.e. decreasing with decreasing shroud clearance. In general, all of the loss components increase with increasing pitch line velocity, so understanding the component mechanisms of windage power loss is critical for the high speed gear trains of modern rotorcraft applications.

## MODIFIED SHROUD TEST RESULTS

Based on the literature review and analysis of the pocketing losses, a windage power loss test was conducted with shrouds modified with cut-outs near the meshing region. Figure 11 shows windage power loss versus pitch-line velocity data for meshed spur gear tests at various shroud configurations. Previous work by the authors in Ref. 5 had shown that the C31 configuration (max. axial, min. radial) condition had given the largest decrease in windage power loss of 29% at a pitch-line velocity of 25,000 ft/min relative to the unshrouded configuration. The C1 configuration, (min. axial, min. radial) decreased WPL by only 13%. Now included in the dataset is windage power loss data for a modified shroud configuration, 'C1mod1', containing square openings at both ends of the meshing spur gears. Compared to the unshrouded configuration at the same pitch-line velocity, a 38% reduction in windage power loss is observed. The axial and radial locations are the same for the C1 and the C1mod1 configuration with the exception of the square-hole cut-outs for the C1mod1 configuration. Results of the modified shroud with cut-outs are indicative of the negative effects of axial jetting. More work is needed to understand axial jetting and how best to mitigate its effect on windage power loss.

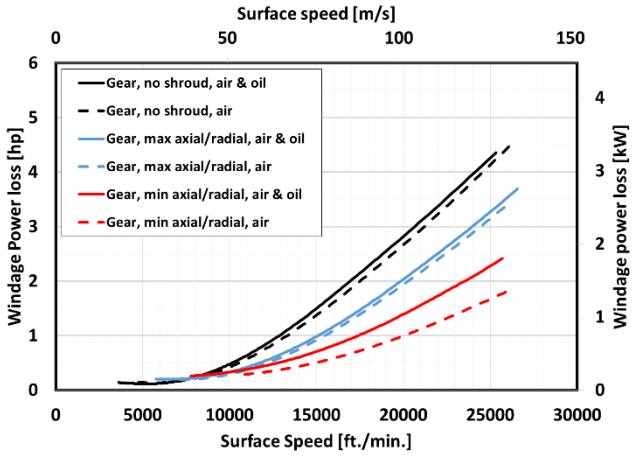


**Figure 10 Single spur gear windage power loss data for various shroud configurations.**

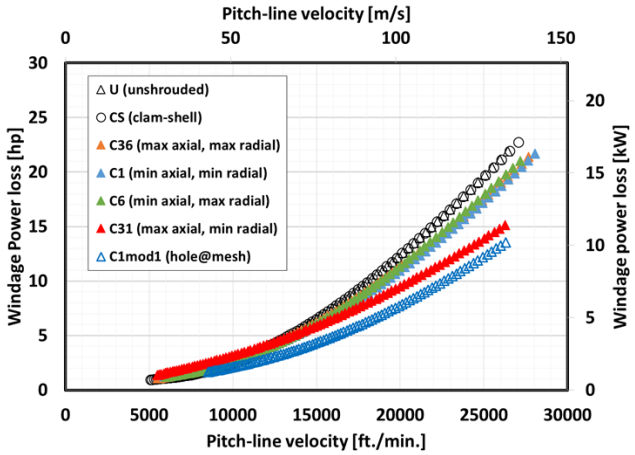


**Figure 11 Meshed spur gear windage power loss data for various shroud configurations.**

## CONCLUSIONS

Results of the literature review showed several analyses and experiments indicating the presence of axial jetting. Although highly dependent on factors such as gear geometry and pitch-line velocity, there was general agreement that axial jetting was found to occur prior to the pitch point and could reach sonic conditions. In addition a 'suction' action occurs

after reaching the pitch point in the meshing cycle. Its effect on windage power loss as well as shrouding is unknown.

A pocketing analysis when compared to NASA windage power loss data found potentially two additional components to windage power loss, 1) an interaction between the meshing spur gears, and 2) a recirculation of the fluid within the interspaces of the gear teeth.

The initial test results for the modified shroud configuration are promising. A 38% reduction in WPL was observed compared to the unshrouded configuration. This is an improvement over the 29% WPL reduction for the maximum axial, minimum radial shroud configuration. Results are indicative of the effect of jetting in the meshing region. Further analysis on the C1mod1 shroud configuration is necessary to optimize the design. From the literature and our tests, a number of design guidelines would aid the shroud optimization.

1) These guidelines would apply for pitch-line velocities higher than 10,000 ft/min.
2) To the degree possible, avoid recirculation of the air/oil mixture in the meshing region.
3) For spur gears, allow for a means of the fluid flow to exit the meshing region in the axial direction.
4) Allow lubricant to cool and lubricate quickly and to exit the meshing region as quickly as possible.
5) These guidelines would apply to the position of oil drains in the gearbox that would allow the quick exit of the lubricant.

## FURTHER WORK

A fluid dynamics model of the gearbox using shrouds at running condition could potentially show the magnitude and direction of the fluid flow and impingement of the air/oil mixture on the gear teeth. Given these results, appropriate shroud modifications could be made that inhibit the air/oil mixture from recirculating back into the gear mesh, teeth, and gear sides. Again the idea here is to limit the fluid to lubrication and cooling of the gears.

Experimental efforts are underway at NASA Glenn Research Center Gear Windage Test Rig to determine the areas of maximum expulsion and suction of the air/lubricant mixture for the spur gears tested by the authors. Dynamic pressure sensors are planned to be used to triangulate the regions of maximum and minimum pressure and to determine end flow velocities from this data. Depending upon the confidence of measurements as well as placement of the sensors next to the spur gear meshing region, a pressure profile map is envisioned that would further aid in understanding the effectiveness of close clearance shrouds.

In addition, a feasibility study is planned of PIV tests of jet-lubricated gears at pitch-line velocities greater than 50 m/s (9843 ft/min). Visual data of this kind, even without shrouding, would greatly increase understanding of the effect of fluid flow within a gearbox in relation to windage power losses.

Author contact:

Irebert Delgado Irebert.R.Delgado@nasa.gov
Michael Hurrell Michael.J.Hurrell@nasa.gov

## ACKNOWLEDGMENTS

The authors acknowledge the support of the NASA Revolutionary Vertical Lift Technology Project and also to Sigurds Lauge (HX5 Sierra LLC) for technical test support.

## REFERENCES

[1] Kahraman, A., D. R. Hilty, and A. Singh. "An experimental investigation of spin power losses of a planetary gear set." Mechanism and Machine Theory 86 (2015): 48-61.

[2] Hill, Matthew J. A Computational Investigation of Gear Windage. The Pennsylvania State University, 2010.

[3] Dudley, D. W., Dudley's Gear Handbook. Ed. Dennis P. Townsend. Tata McGraw-Hill Education, 1991, 12.24.

[4] Diab Y.Y., Ville F.F., Velex P.P., Changenet C.C., "Windage Losses in High Speed Gears—Preliminary Experimental and Theoretical Results," Journal of Mechanical Design, Oct. 2004, Vol. 126, (5), pp. 903-908, doi:10.1115/1.1767815.

[5] Delgado, I., and Hurrell, M., 2017, "The Effectiveness of Shrouding on Reducing Meshed Spur Gear Power Loss – Test Results," AGMA Fall Technical Meeting, Columbus, Ohio.

[6] Rosen MW. Noises of Two Spur-Gear Transmissions. Noise Control. 1961 Nov;7(6):11-9.

[7] Dudley, D. W. (1962). Gear handbook: the design, manufacture, and application of gears. McGraw Hill Higher Education.

[8] Wittbrodt MJ, Pechersky MJ. A hydrodynamic analysis of fluid flow between meshing spur gear teeth. PENNSYLVANIA STATE UNIV UNIVERSITY PARK APPLIED RESEARCH LAB; 1987 Oct.

[9] Diab, Y., Ville, F., Houjoh, H., Sainsot, P., Velex, P. Experimental and numerical investigations on the air-pumping phenomenon in high-speed spur and helical gears. Proceedings of the Institution of Mechanical Engineers, Part C: Journal of Mechanical Engineering Science. 2005 Aug 1;219(8):785-800.

[10] Seetharaman S, Kahraman A. A windage power loss model for spur gear pairs. Tribology Transactions. 2010 Jul 16;53(4):473-84.

[11] Ariura, Y., Ueno, T., Sunaga, T., and Sunamoto, S. The lubricant churning loss in spur gear systems. Bulletin of JSME. 1973;16(95):881-9

[12] Concli F, Gorla C. Oil squeezing power losses in gears: a CFD analysis. WIT Transactions on Engineering Sciences. 2012 Jun 26;74:37-48.

[13] Al, B.C., Simmons, K., Morvan, H.P.. Computational investigation of flows and pressure fields associated with spur gear meshing. InASME Turbo Expo 2014: Turbine Technical Conference and Exposition 2014 Jun 16 (pp. V05CT16A023-V05CT16A023). American Society of Mechanical Engineers.

[14] Burberi, E., Fondelli, T., Andreini, A., Facchini, B., Cipolla, L. CFD Simulations of a Meshing Gear Pair. InASME Turbo Expo 2016: Turbomachinery Technical Conference and Exposition 2016 Jun 13 (pp. V05AT15A024-V05AT15A024). American Society of Mechanical Engineers.

[15] Gorla, C., Concli, F., Stahl, K., Höhn, B.R., Michaelis, K., Schultheiß, H., Stemplinger, J.P. Hydraulic losses of a gearbox: CFD analysis and experiments. Tribology International. 2013 Oct 1;66:337-44.

[16] Hartono, E., Golubev, M., & Chernoray, V. (2013). PIV Study of Fluid Flow Inside A Gearbox. In PIV13; 10th International Symposium on Particle Image Velocimetry, Delft, The Netherlands, July 1-3, 2013.

[17] Hartono, E. A., Pavlenko, A., & Chernoray, V. (2014). Stereo-PIV Study of Oil Flow Inside a Model Gearbox. In 17th International Symposium on Applications of Laser Techniques to Fluid Mechanics (pp. 07-10).

[18] Delgado, I., and Hurrell, M., 2017, "Experimental Investigation of Shrouding on Meshed Spur Gear Windage Power Loss," AHS International 73rd Annual Forum and Technology Display, Ft. Worth, Texas.

[19] Petry-Johnson, T. T., Kahraman, A., Anderson, N. E., & Chase, D. R. (2008). An experimental investigation of spur gear efficiency. Journal of Mechanical Design, 130(6), 062601.

[20] Merritt, H. E. (1971). Gear engineering. John Wiley & Sons.

[21] Engeda, A., Raheel, M. Theory and Design of the Regenerative Flow Compressor. Proceedings of the International Gas Turbine Congress, November 2-7, 2003.